Electronic Supplementary Information

The influences of the transfer method and particle surface chemistry on the dispersion of nanoparticles in nanocomposites

Olivier Pravaz,[a] Benoît Droz,[b] Peter Schurtenberger[c] and Hervé Dietsch*[a,d]

[a]*University of Fribourg, Adolphe Merkle Institute and Fribourg Center for Nanomaterials, P.O. box 209, 1723 Marly 1, Switzerland. E-mail: herve.dietsch@gmail.com.*
[b]*Nanonet & College of Engineering and Architecture of Fribourg, P.O. box 32, 1705 Fribourg, Switzerland.*
[c]*Physical Chemistry 1, University of Lund, Sweden. E-mail: peter.schurtenberger@fkem1.lu.se*
[d]*Current address: BASF SE, Formulation Platform, 67056 Ludwigshafen am Rhein, Germany. E-mail: herve.dietsch@basf.com.*

1. Characterizations of the nanoparticles.

The nanoparticle (NP) synthesis resulted in a dispersion in ethanol that was stable over several months. Typical electron microscopy images of the particles are shown in Figure S1. On the analysis of the electron microscopy pictures results in a mean radius (R) of 24.2 ± 3.2 nm (Figure S1) while, dynamic light scattering (DLS) provides mean hydrodynamic radii (R_h) of 30 ± 5 nm for bare silica and 31 ± 8 nm for the surface modified ones. Elemental analysis reveals a grafting density of the TPM coupling agent of 3.2 nm^{-2}. The form factor of the fillers was extracted from SAXS measurements on dilute samples of fillers in solution ($\varphi = 0.01$). The intensity of scatterers in a medium is proportional to the form of fillers and their organization inside the matrix and is expressed as $I(q) = n\Delta\rho^2 V^2 P(q) S(q)$. With n the number density, $\Delta\rho$ the difference in scattering length density between NPs and solvent/matrix, V the volume of the filler, and $P(q)$ and $S(q)$ are respectively the effective form and structure factors. When the concentration of NPs is low enough, there are no positional correlations which implies $S(q) = 1$. Figure S2 shows the resulting scattering curves for bare silica and TPM-coated silica NPs in ethanol together with form factors for homogeneous spheres[1] (dashed lines) and the best fits obtained (full lines). For bare NPs, large deviations from the form factor and the scattering intensity are visible at low q-values (Figure S2). This is characteristic for the presence of larger objects. The curve can indeed be well fitted by a combination of a form factor for spheres having a mean radius $R_1 = 24.5 \pm 3.2$ nm together with a second one for spheres with $R_2 = 34.0 \pm 10.2$ nm representing less than 3 % in number. Both populations are assumed to have a

log-normal distribution. The presence of big particles is attributed to the aggregation of nuclei resulting in the formation of doublets during the synthesis and to the aggregation of a few NPs in solution. Some of these particles are visible on the TEM images and are highlighted by circles in the inset of Figure S1. A Guinier plot (Figure S2 inset) shows a break in the slope at very low q values ($q^2 < 3.10^{-5}$ A^{-2}) also pointing to the presence of some aggregates. The two slopes are related to two characteristic sizes in the silica population, and the calculated sizes (R_{g1} = 23.2 nm & R_{g2} = 32.2 nm) are in good agreement with the ones found from TEM and DLS data. To correct for the contribution from the small aggregates in the fitting model, only the form factor corresponding to the main size and polydispersity of the fillers (dashed line) is used for the structure factor calculations. For TPM-coated NPs, the SAXS curve shows only minor deviations from the form factor in the Guinier region. This deviation is due to residual correlation effects[2] ($S(q)$) in the scattering intensity for very low q values even at this low loading (~ 1 vol%). The additional TPM coating layer tends to slightly increase the mean radius up to R = 25.0 ± 3.2 nm, in accordance with the DLS measurements.

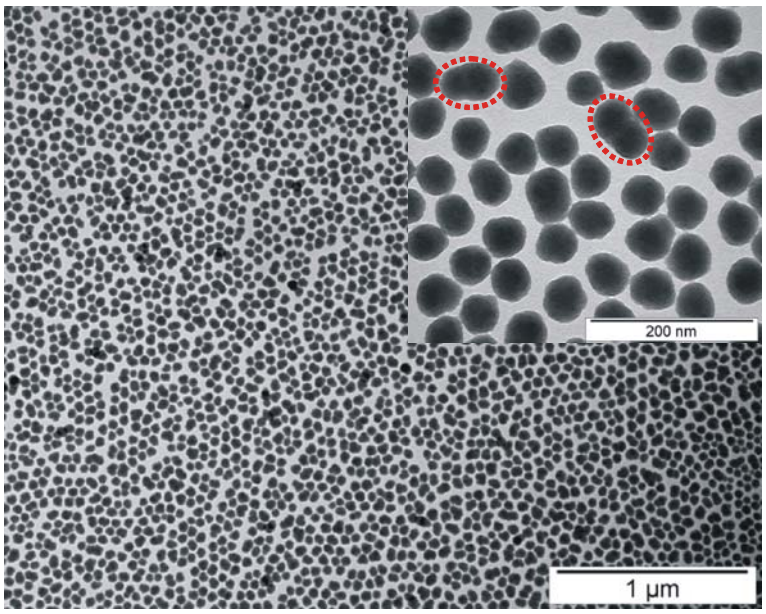

Figure S1: TEM images of Stöber silica nanoparticles at different magnifications. Dashed circles show examples of nanoparticles with shape and size deviations from mean spheres.

For both bare and TPM-coated NPs, deviations from the typical behavior of solid homogeneous spheres are observed in the Porod-region. For $q > 0.5$ nm^{-1}, the scattering intensity exhibits a power law behavior $I \sim q^{-2.8}$ instead of $I \sim q^{-4}$, due to the high porosity of the nanoparticles.[3,4] A mean radius of gyration for the pores of R_{gp} = 3.0 ± 0.8 nm, assuming that they are aggregated with a fractal dimension (D) of 2.8, is necessary to properly fit the Porod-region for both systems. The scattering contribution for pores is expressed by a mass fractal expression like $I_p(q) = \frac{\sin\left[(D-1)\arctan(q\xi)\right]}{(D-1)q\xi\left(1+q^2\xi^2\right)^{(D-1)/2}}$; where ξ corresponds to the linear size of aggregates and is

proportional to $\left(\frac{2R_g^2}{D(D+1)}\right)^{1/2}$.[5,6] The porosity of the silica surface is also seen in a BET characterization,[7] which yielded an average pore radius (R_p) of 3.0 nm. The specific surface area (S), and the total volume of pores (V_p) are determined to be 285.0 $m^2.g^{-1}$ and 0.43 $cm^3.g^{-1}$, respectively.

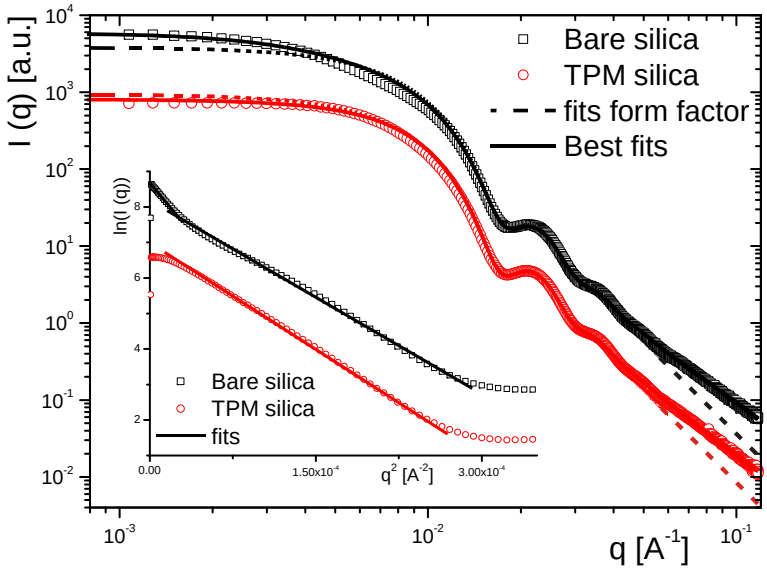

Figure S2: SAXS curves of bare and TPM-coated silica nanoparticles with fits of form factors (dash lines) and best fits (full lines) for highly porous hard spheres with log-normal size distributions. Inset shows corresponding Guinier plots.

2. Highly magnified microtomed TEM images of TPM-coated NPs in PMMA similar to Fig. 5.

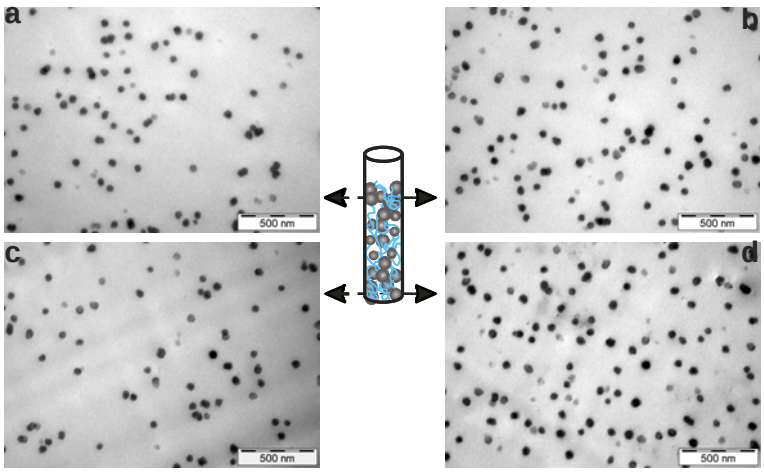

Figure S3: High magnification of microtomed TEM images (80 nm thick) of TPM-coated Silica NPs in the PMMA matrix. (a&b) from the upper part of the samples, while (c&d) are from the lower part of the samples. (a&c) Dried Hybrid Polymer and (b&d) Centrifuged Hybrid Polymer.

3. References.

1. L. Rayleigh, Proceedings of the Royal Society A, 1911 **84**, 25-38.
2. J. S. Meth, S. G. Zane, C. Chi, J. D. Londono, B. A. Wood, P. Cotts, M. Keating, W. Guise and S. Weigand, Macromolecules, 2011, **44**, 8301-8313.
3. M. Reufer, H. Dietsch, U. Gasser, A. Hirt, A. Menzel and P. Schurtenberger, The Journal of Physical Chemistry B, 2010, **114**, 4763-4769.
4. D. W. Schaefer, Science, 1989, **243**, 1023-1027.
5. D. W. Schaefer and K. D. Keefer, Physical Review Letters, 1986, **56**, 2199-2202.
6. M. Foret, J. Pelous and R. Vacher, Journal de Physique 1 France, 1992, **2**, 791-799.
7. S. Brunauer, P. E. Emmett and E. Teller, Journal of the American Chemical Society, 1938, **60**, 309-319.